Influence of Indenter Geometry on the Deformation Behavior of $Zr_{60}Cu_{30}Al_{10}$ Bulk Metallic Glass during Nanoindentation

Byung-Gil Yoo[1], Ju-Young Kim[2], Jae-il Jang[1,*]

[1]*Division of Materials Science and Engineering, Hanyang University, Seoul 133-791, Korea*
[2]*School of Materials Science and Engineering, Seoul National University, Seoul 151-744, Korea*

As a first step in examining a new aspect of inhomogeneous plastic flow in bulk metallic glasses (BMGs) during nanoindentation, a series of nanoindentation experiments were performed on $Zr_{60}Cu_{30}Al_{10}$ BMG with two pyramidal indenters (Berkovich and cube-corner indenters) having different centreline-to-face angle. It was revealed that the indenter angle can be a new controllable factor affecting the serrated flow behaviour of the BMG during nanoindentation, since a sharper cube-corner indenter induces different stress field under the contact from Berkovich indenter typically used. Results are discussed in terms of preliminary ideas for improving analysis of the shear-band-ruled deformation behaviours in the BMG during nanoindentation. [doi:10.2320/matertrans.MJ200752]

1. Introduction

In bulk metallic glasses (BMGs), plastic strain is highly localized into very narrow regions (so-called 'shear bands') at room temperature or a temperature significantly below the glass transition temperature (T_g).[1] This unique and interesting plastic deformation behavior of the metallic glasses at room temperature has been of great scientific interests over the past two decades (even before it became possible to produce them in bulk form). Recently research in the field has accelerated with advances in instrumented load- and depth-sensing indentation techniques (especially, nanoindentation[2,3]) that made it possible to investigate the mechanical response during the entire loading sequence. Numerous nanoindentation studies have examined the shear-band-ruled deformation behavior and mechanisms in BMGs, as well reviewed by Schuh and Nieh.[4] One of the topics often highlighted by nanoindentation studies on BMGs is the inhomogeneous plastic flow observed during indentation experiments. Since Wang *et al.*[5] reported a few small discrete steps (so-called 'pop-ins') in nanoindentation load-displacement (*P-h*) curves of Zr-Al-Ti-Cu-Ni BMG, many works have been focused on the unique feature of the 'pop-ins' and 'serrations' in loading curve of the BMGs during nanoindentation.[6–17] Systematic work on the topic by Schuh, Nieh and their colleagues[8–12] demonstrated that the serrated (inhomogeneous) plastic flow of the BMG during nanoindentation is strongly dependent not only on chemical composition but also on indentation loading rate; the serrated flow is observed only at a slow loading rate and it gradually disappears with increasing loading rate.

Here, in addition to the loading-rate dependency often examined in the past, we introduce a somewhat new indentation parameter to study the serrated behavior in a Zr-based BMG: the geometry (sharpness) of the pyramidal indenter as characterized by centerline-to-face angle. By applying two indenters with different angles (the commonly used Berkovich indenter and a sharper cube-corner indenter),

it was found that serrated flow behavior also depends significantly on indenter angle (i.e., indenter sharpness) and thus that a cube-corner indenter can be very helpful in investigating the serrations in the *P-h* curve of BMGs.

2. Experimental

Nanoindentations were made on a $Zr_{60}Cu_{30}Al_{10}$ bulk metallic glass (prepared by arc melting followed by drop casting) using a Nanoindenter-XP (MTS Corp., Oak Ridge, TN) with two different triangular pyramidal diamond indenters having centerline-to-face angles of 65.3° (Berkovich indenter) and 35.3° (cube-corner indenter). The maximum indentation loads (P_{max}) were 10 and 100 mN, and loading rates (dP/dt) varied from 5 to 0.05 mN/s. In order to capture the serrated flow behavior properly, thermal drift was maintained below 0.05 nm/s. More than five indentation tests under each testing condition were carried out on the sample which was mechanically polished to a mirror finish.

After nanoindentation testing, hardness impressions were observed by field emission scanning electron microscopy (FE-SEM) JSM-6330F (JEOL, Japan), and the profiles of the indented surfaces were examined by atomic force microscopy (AFM) XE-100 (PSIA, Suwon, Korea).

3. Results and Discussion

Figure 1 shows representative load-displacement (*P-h*) curves observed during nanoindentation to relatively high and low peak loads ($P_{max} = 100$ mN and 10 mN) with a Berkovich indenter at a variety of loading rates dP/dt (from 0.05 mN/s to 5 mN/s). Each *P-h* curve has been shifted for clarity of presentation. During slow indentation (i.e., low dP/dt), the loading curves are serrated by a series of discrete steps ('pop-ins') where the indentation displacement increases rapidly at a given load. As the loading rate increases, the discrete events disappear in the low load regime (Fig. 1(a)) or change to a small 'ripples' in the high load regime (Fig. 1(b)). This apparent rate-dependency of the serrations in the *P-h* curve is in good agreement with

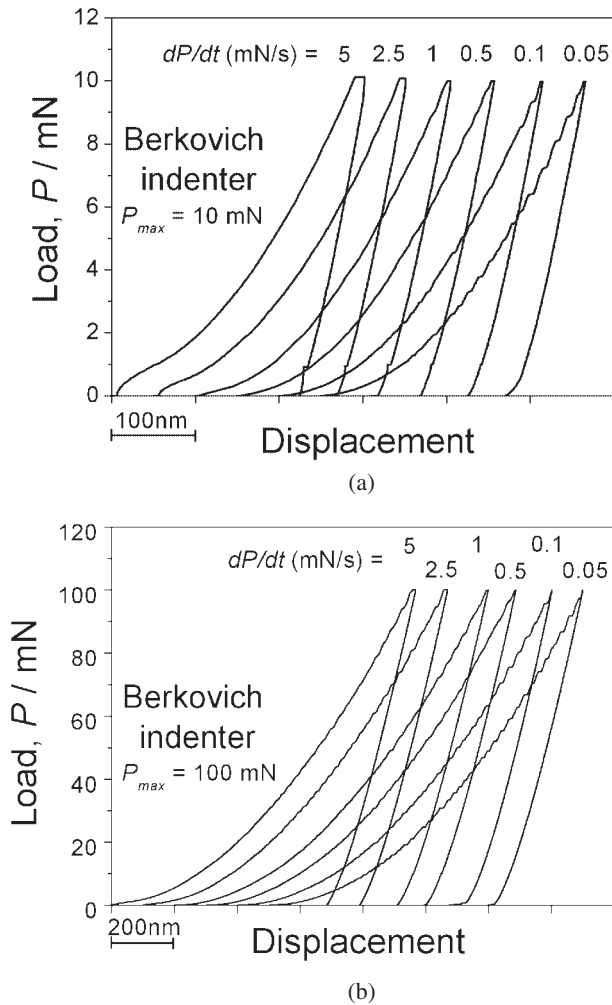*Corresponding author, E-mail: jijang@hanyang.ac.kr

Fig. 1 Typical load-displacement curves obtained from nanoindentations with Berkovich indenter at various loading rates, dP/dt, and maximum indentation load: P_{max} = (a) 10 mN and (b) 100 mN.

Fig. 2 Representative examples of load-displacement curves obtained from nanoindentations made with cube-corner indenter at various loading rates, dP/dt, and maximum indentation load: P_{max} = (a) 10 mN and (b) 100 mN.

previous research on various BMGs.[8–17] In Fig. 1(a), the abnormal shape of the early part of the loading curve under fast loading may be due to the low data acquisition rate and insufficient instrumental resolution at such a high loading rate.[13,14]

It is noteworthy that in the prior works, the rate-dependent serrated flow phenomena have been more clearly observed in some BMGs such as Pd-based BMGs[4,6,8,10–13] (which also showed obvious serrations in stress-strain curves from compressive tests[18]) than in other BMGs such as Zr-based ones, which can be simply interpreted as the dependency of the discrete deformation on the chemical compositions of the BMGs tested. For examples, in a review by Schuh and Nieh,[4] a $Zr_{65}Al_{10}Ni_{10}Cu_{15}$ BMG (whose composition is a little similar to that of the ternary BMG used here) showed the least pronounced serrations in the P-h curve of all the BMGs examined. Also, some researchers have observed few or no distinguishable discontinuities in the P-h curves of Zr-based BMGs;[4,13,17,19] this is possibly associated with the low indentation loads applied in the studies. In Fig. 1, the displacement discontinuities increases in size with increasing load or displacement. This implies that due to the nature of the geometrically self-similar sharp indenter, the amount of
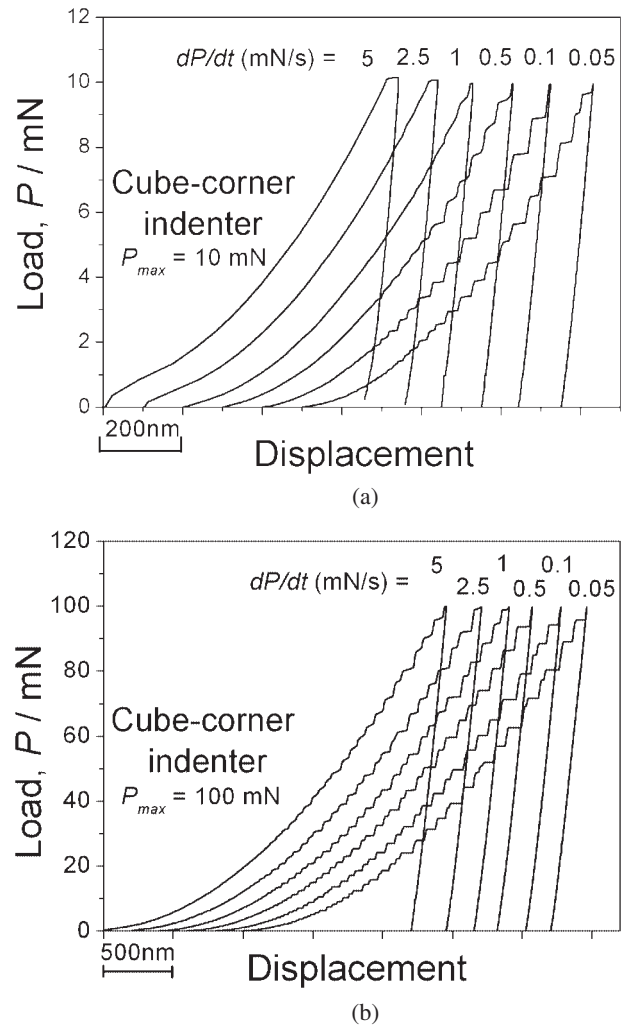
strain accommodation by each pop-in is constant and independent of load level. Hence, for clearer observations of the serrations, at first, one might need to increase the indentation peak load to level high enough.

A new way to enhance the resolvability of the serrated deformation behavior can be found in Fig. 2, which shows typical P-h curves recorded during nanoindentation with a cube-corner indenter at various loading rates. As seen in the figure, the sharper cube-corner indenter produces a larger peak-load displacement and a greater proportion of permanent plastic deformation after unloading (i.e., a higher ratio of final displacement to maximum displacement, h_f/h_{max}) than the Berkovich indenter. The most important feature in comparing Figs. 1 and 2 is the far more pronounced discrete horizontal steps during cube-corner indentation than during Berkovich indentation (the latter shows 'ripples' rather than the 'pop-ins' of the former). The rate dependency of serrated flow in the P-h curve for Berkovich indentation is also seen in the cube-corner indentation; the slow indentations exhibit clearer serrations in P-h curves than the fast indentations. This result suggests that the serrated flow behavior depends not only on loading rate but also on the indenter angle,
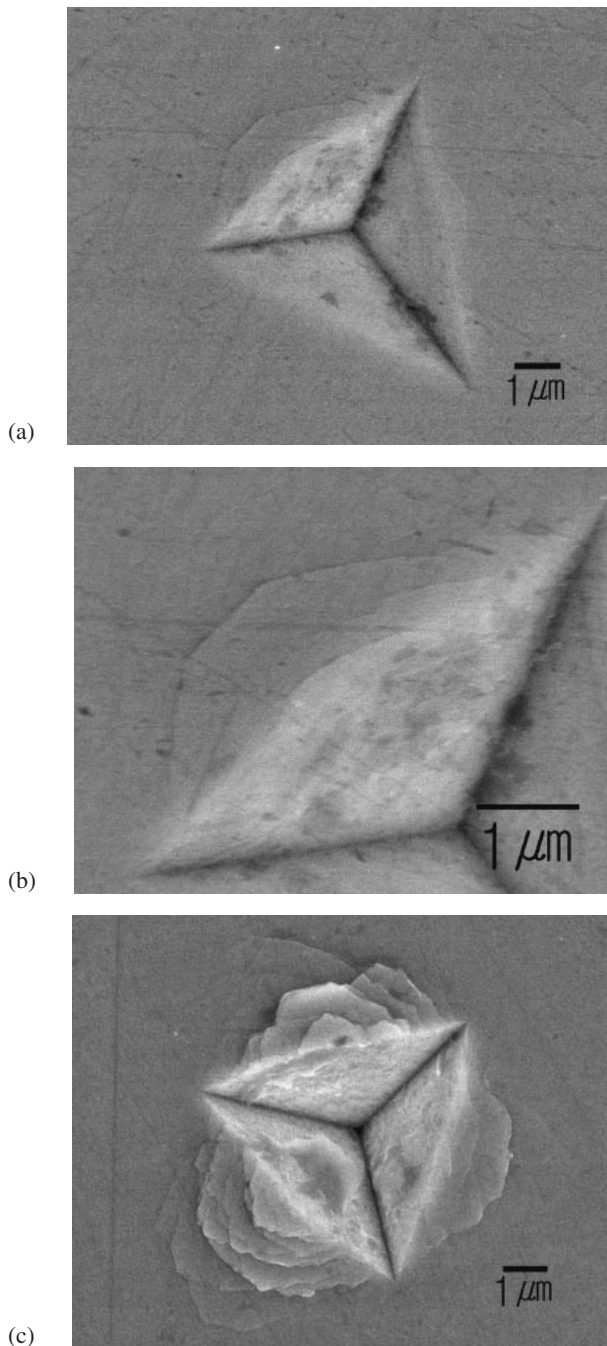
(a)

(b)

(c)

Fig. 3 SEM micrographs of hardness impressions of different pyramidal indenters at $P_{max} = 100$ mN and $dP/dt = 0.05$ mN/s: (a) from Berkovich indentation; (b) part of (a) magnified for clarity of shear bands; (c) from cube-corner indentation. Note that the magnifications of images (a) and (c) are not exactly the same.

implying that use of a cube-corner indenter may be very helpful in analyzing the serration phenomena in BMGs.

Typical SEM images of hardness impressions made at relatively high load ($P_{max} = 100$ mN) and the lowest loading rate ($dP/dt = 0.05$ mN/s) are shown in Fig. 3. Interestingly, there is obvious difference between the Berkovich and cube-corner indentations: while only a few distinct shear bands are seen around Berkovich indentations (Figs. 3(a) and 3(b)), many discrete circular shear bands appear around the indent produced by the cube-corner indenter (Fig. 3(c)). The more pronounced serrations in the P-h curves and shear bands

extrusion in the SEM image for cube-corner indenter might be an evidence for a strong relationship between the loading curve shape and the actual deformation; many pop-ins in the P-h curve indeed correspond to shear band activity as previously suggested.[4,7–17]

It is interesting to point out that only a few shear bands are seen in the pile-up area around the Berkovich indentation, although the serrations are clearly observed at the same testing condition, $dP/dt = 0.05$ mN/s and $P_{max} = 100$ mN (Fig. 1(b)). One possibility is that for Berkovich indentation, the shear bands are captured beneath the indent and cannot emerge to the surface. Very recently, Li $et\ al.$[17] showed from cross-sectional SEM observations of the indent in a Zr-Al-Ni-Cu-Be BMG (prepared by an interface bonding technique) that a large number of semicircular shear bands form in the deformation zone beneath the Vickers indenter but do not propagate to the upper surface of the sample.

The next question, thus, is why explosive extrusion of shear bands around the impression of a cube-corner indenter does not occur with a Berkovich indentation. One might gain some insights from previous work[20,21] on extrusion phenomena in semiconductor materials during nanoindentation, which is somewhat analogous to the observations here. In semiconductor materials such as silicon (whose dominant deformation during indentation is not by dislocation activity but by indentation-induced phase transformation), transformed ductile-phase material was extruded around the indent only in relatively sharp cube-corner indentation, not in Berkovich indentation. According to Sneddon's comprehensive model[22] for elastic contact by a rigid cone, the distribution of pressure (p) under the indenter is given by

$$p(r) = \frac{E}{2(1 - \nu^2)} \frac{\cosh^{-1}(a/r)}{\tan \Psi}, \quad 0 \leq r \leq a \qquad (1)$$

where ψ is the half cone angle, E is Young's modulus, ν is Poisson's ratio, a is the contact radius, and r is the radial coordinate on the surface. This equation suggests that in elastic contact, higher pressures are sustained on larger fractions of the contact radius for indenters with smaller angles. Thus, for the cube-corner indenter with much smaller angle, sufficiently high pressure over the critical stress required for shear-bands formation/propagation is distributed over a 'greater fraction' of the contact area (i.e., higher r/a) beneath the indenter during elastic contact than for the Berkovich indenter. In BMG, the critical pressure for shear banding can be approximately the same as the hardness, if there is no work hardening. Thus, the possibility that the shear bands can escape from under the contact to the free surface at the contact edge is greater for the sharp cube-corner indenter. For the Berkovich indenter, since the high-pressure region (where shear bands can form and propagate) is relatively small, flow by shear bands propagation is inhibited by the surrounding low-pressure regions.

A further advantage of indentation testing with two pyramidal indenters of different angles is that one might acquire baseline information on macroscopic stress-strain relationships in the plastic deformation regime. Three-sided pyramidal indenters such as Berkovich and cube-corner indenters are geometrically self-similar and thus have their own characteristic stress and strain values that may corre-

Table 1 Averaged hardness values measured at different loading rates with Berkovich and cube-corner indenters.

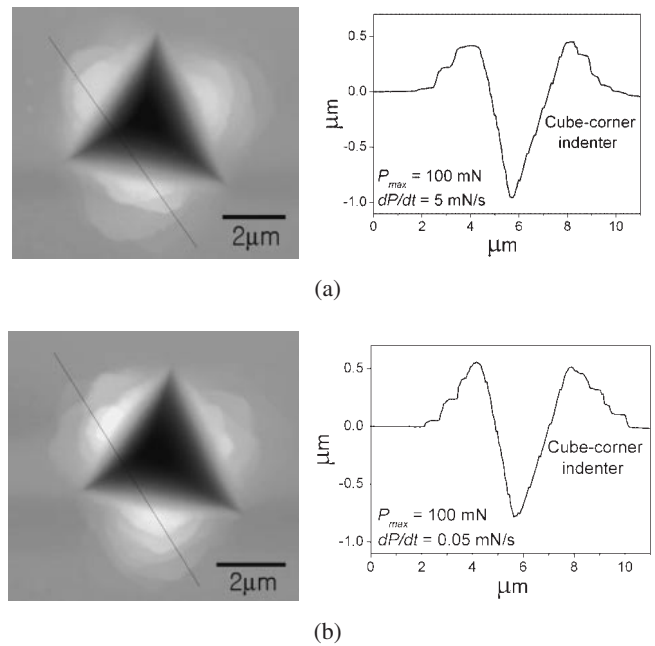| Indenter type	Loading rate			
	5 mN/s	1 mN/s	0.5 mN/s	0.05 mN/s
Berkovich indenter ($\Psi = 65.3°$)	6.17 GPa	6.24 GPa	6.76 GPa	6.54 GPa
Cube-corner indenter ($\Psi = 35.3°$)	6.86 GPa	6.58 GPa	6.51 GPa	6.43 GPa

(a)

(b)

Fig. 4 AFM images and corresponding depth profiles obtained from indentation impressions made with a cube-corner indenter at $P_{max} = 100$ mN and $dP/dt =$ (a) 5 mN/s and (b) 0.05 mN.

spond to a single point on the macroscopic true stress vs. true strain curve for the same material. Since Atkins and Tabor[23] demonstrated experimentally that hardness values of copper and mild steel change dramatically with indenter angle, there have been many efforts to obtain stress-strain curves directly from indentations with sharp indenters of different angles.[24–27] Although a quantitative definition of the characteristic strain for each indenter angle has not been fully established, it is well accepted that the characteristic strain for a cube-corner indenter is much greater than that for Berkovich indenter. Therefore, by comparing hardness values from cube-corner indentation and Berkovich indentation, it is possible roughly to predict the shape of the plastic regime in the macroscopic tensile (true stress vs. true strain) curve of BMG materials, which is still hard to measure by conventional mechanical testing. Because the typical nanoindentation hardness measurement method suggested by Oliver and Pharr[2,3] cannot be simply applied to BMGs that show severe material pile-up around the indent,[28] here we measure the area of residual hardness impressions directly using SEM images and estimate the hardness from that. Table 1 lists the averaged hardness values measured in this work, which seem almost independent of indenter angle as well as loading rate. Thus, the macroscopic plastic behavior of this Zr-Cu-Al BMG is expected to be fully plastic.

One still unresolved question is raised by the AFM images of the cube-corner indentations in Fig. 4. Jiang and Aztmon[14] showed experimentally that rate-dependent serration behavior results in a rate-dependent shear-band density (i.e., higher shear-band density at faster loading). However, in this work, this tendency is unclear; indeed, at times the opposite trend was observed (see Fig. 4). Further studies focused on shear band density not only on the surface but also beneath the indenter are thus desirable.

4. Conclusions

We explored the shear-band-ruled deformation behavior of $Zr_{60}Cu_{30}Al_{10}$ BMG during nanoindentation with two geometrically different pyramidal indenters (Berkovich indenter and a relatively sharper cube-corner indenter). The results revealed strong dependence of serrated flow behavior on indenter angle as well as indentation loading rate; discrete deformations are more pronounced for sharper indenters and lower loading rates. This means that the sharper cube-corner indenter might be very useful in analyzing the serrated flow behavior of BMGs. Additionally, by comparing the hardness from cube-corner and Berkovich indentation, we could roughly estimate the macroscopic shape of the stress-strain curve, which seems to be approximately fully plastic in the Zr-Cu-Al BMG examined here.

Acknowledgement

REFERENCES

1) F. Spaepen: Acta Metall. **25** (1977) 407–415.
2) W. C. Oliver and G. M. Pharr: J. Mater. Res. **7** (1992) 1564–1583.
3) W. C. Oliver and G. M. Pharr: J. Mater. Res. **19** (2004) 3–20.
4) C. A. Schuh and T. G. Nieh: J. Mater. Res. **19** (2004) 46–57.
5) J. G. Wang, B. W. Choi, T. G. Nieh and C. T. Liu: J. Mater. Res. **15** (2000) 798–807.
6) Y. I. Golovin, V. I. Ivolgin, V. A. Khonik, K. Kitagawa and A. I. Tyurin: Scripta Mater. **45** (2001) 947–952.
7) A. L. Greer and I. T. Walker: Mater. Sci. Forum **386–388** (2002) 77–88.
8) C. A. Schuh, T. G. Nieh and Y. Kawamura: J. Mater. Res. **17** (2002) 1651–1654.
9) T. G. Nieh, C. Schuh, J. Wadsworth and Y. Li: Intermetallics **10** (2002) 1177–1182.
10) C. A. Schuh and T. G. Nieh: Acta Mater. **51** (2003) 87–99.
11) C. A. Schuh, A. S. Argon, T. G. Nieh and J. Wadsworth: Phil. Mag. **83** (2003) 2585–2597.
12) C. A. Schuh, A. C. Lund and T. G. Nieh: Acta Mater. **52** (2004) 5879–5891.
13) A. L. Greer, A. Castellero, S. V. Madge, I. T. Walker and J. R. Wilde: Mater. Sci. Eng. A **375–377** (2004) 1182–1185.
14) W. H. Jiang and M. Atzmon: J. Mater. Res. **18** (2004) 755–757.
15) B. C. Wei, T. H. Zhang, W. H. Li, Y. F. Sun, Y. Yu and Y. R. Wang: Intermetallics **12** (2004) 1239–1243.
16) A. Concustell, J. Sort, G. Alcala, S. Mato, A. Gebert, J. Eckert and M. D. Baro: J. Mater. Res. **20** (2005) 2719–2725.

17) W. H. Li, T. H. Zhang, D. M. Xing, B. C. Wei, Y. R. Wang and Y. D. Dong: J. Mater. Res. **21** (2006) 75–81.
18) P. E. Donovan: Acta Metall. **37** (1989) 445–456.
19) R. Vaidyanathan, M. Dao, G. Ravichandran and S. Suresh: Acta Mater. **49** (2001) 3781–3789.
20) J.-I. Jang, M. J. Lance, S. Wen, T. Y. Tsui and G. M. Pharr: Acta Mater. **53** (2005) 1759–1770.
21) J.-I. Jang, M. J. Lance, S. Wen and G. M. Pharr: Appl. Phys. Lett. **86** (2005) Art. No. 131907.
22) I. N. Sneddon: Int. J. Eng. Sci. **3** (1965) 47–57.

23) A. G. Atkins and D. Tabor: J. Mech. Phys. Solids **13** (1965) 149–164.
24) K. L. Johnson: J. Mech. Phys. Solids **18** (1970) 115–126.
25) Y.-T. Cheng and Z. Li: J. Mater. Res. **15** (2000) 2830–2835.
26) N. Chollacoop, M. Dao and S. Suresh: Acta Mater. **51** (2003) 3713–3729.
27) J. L. Bucaillle, S. Stauss, E. Felder and J. Michler: Acta Mater. **51** (2003) 1663–1678.
28) W. J. Wright, R. Saha and W. D. Nix: Mater. Trans., JIM **42** (2001) 642–649.